ACS Macro Letters

Letter

pubs.acs.org/macroletters

Surface-Sensitive Approach to Interpreting Supramolecular Rearrangements in Cellulose by Synchrotron Grazing Incidence Small-Angle X-ray Scattering

Heike M. A. Ehmann,*[,†] Oliver Werzer,[‡] Stefan Pachmajer,[⊥] Tamilselvan Mohan,[§] Heinz Amenitsch,[∥] Roland Resel,[⊥] Andreas Kornherr,[◆] Karin Stana-Kleinschek,[#] Eero Kontturi,*[,∇,○] and Stefan Spirk*[,#,†,¶]

[†]Institute for Chemistry and Technology of Materials, Graz University of Technology, Stremayrgasse 9, A-8010 Graz, Austria

[‡]Institute of Pharmaceutical Science, Department of Pharmaceutical Technology, Karl-Franzens University of Graz, Universitätsplatz 1, A-8010 Graz, Austria

[§]Institute for Chemistry, Karl-Franzens University of Graz, Heinrichstraße 28, A-8010 Graz, Austria

[∥]Institute of Inorganic Chemistry, Graz University of Technology, Stremayrgasse 9, A-8010 Graz, Austria

[⊥]Institute of Solid State Physics, Graz University of Technology, Petersgasse 16, A-8010 Graz, Austria

[#]Institute for Engineering Materials and Design, University of Maribor, Smetanova ulica 17, SI-2000 Maribor, Slovenia

[∇]Polymer and Composites Engineering group, Department of Forest Products Technology, Aalto University, PO Box 16300, FI-00076 Aalto, Finland

[○]Department of Chemical Engineering, Imperial College London, South Kensington Campus, London SW7 2AZ, U.K.

[◆]Mondi Uncoated Fine & Kraft Paper GmbH, Marxergasse 4A, 1030 Wien, Austria

Supporting Information

ABSTRACT: The supramolecular rearrangements of biopolymers have remained difficult to discern. Here, we present a versatile approach that allows for an *in situ* investigation of two major types of rearrangements typically observed with cellulose, the most abundant biopolymer on earth. Model thin films were employed to study time-resolved pore size changes using *in situ* grazing incidence small-angle X-ray scattering (GISAXS) during regeneration and drying.

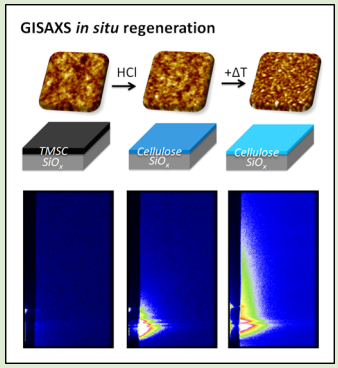

Many aspects of supramolecular rearrangements of various biopolymers have remained elusive despite significant advances in modern analytical techniques like NMR spectroscopy, electron microscopies, and many of the scattering techniques. One of the challenging cases is cellulose, the load-bearing molecule in all plants, thereby accounting for the largest share among all available biopolymers on earth.[1] Although the molecular structure of cellulose is that of a linear homopolymer consisting of anhydroglucose units (Figure 1a), its supramolecular structure has provided formidable challenges for researchers over the years.[2] Thanks to intensive efforts utilizing, for example, neutron and X-ray scattering, electron diffraction, computer simulations, and solid-state NMR spectroscopy, the contemporary knowledge on cellulose structure is on a fairly high level,[3] but many seminal questions still remain.[4] For example, rearrangements between cellulose units upon, e.g., swelling or dissolution and possible subsequent regeneration are a point of debate. Furthermore, the effect of water in a cellulose matrix has been difficult to interpret in the nano/mesoscale level.[5] Particularly, techniques yielding *in situ* data are scarce. The lack of knowledge hampers the use of cellulose in traditional (textiles, paper) as well as modern applications like biofuels, self-healing hydrogels, transistors, chiral templates, or fully biodegradable composites.[6]

In this paper, we present a fresh analytical perspective on following rearrangements in cellulose upon regeneration and subsequent drying, namely, a surface-sensitive approach based on ultrathin films. As the instrumental method, we have chiefly exploited grazing incidence small-angle X-ray scattering (GISAXS) at a synchrotron facility, one of the scattering techniques that has just evolved during the past decades. The utilization of homogeneously amorphous, well-defined ultrathin

Received: May 8, 2015
Accepted: June 19, 2015
Published: June 22, 2015

DOI: 10.1021/acsmacrolett.5b00306
ACS Macro Lett. 2015, 4, 713−716

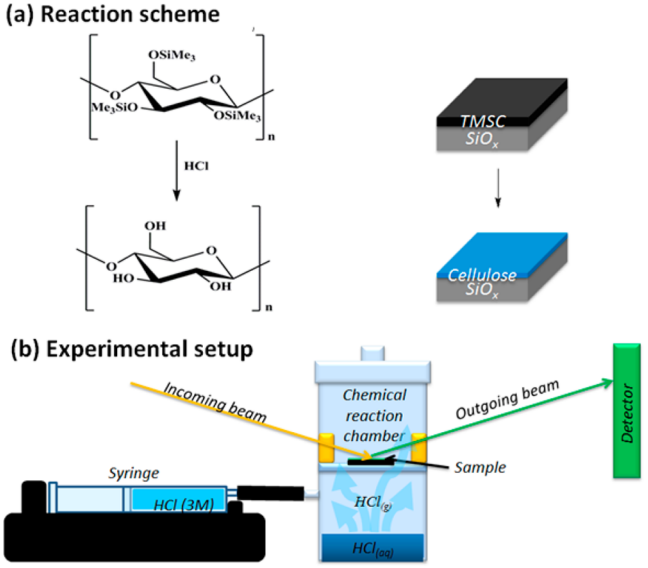

Figure 1. (a) Reaction scheme showing the conversion of trimethylsilyl cellulose to cellulose via HCl vapor hydrolysis. Note that the TMSC has a degree of substitution with TMS groups of 2.5. (b) Schematic experimental setup of the *in situ* regeneration using GISAXS. The incidence angle was set to 0.76°.

films circumvents several problems associated with characterization of cellulose or many other biopolymers like the heterogeneity in morphology and supramolecular as well as chemical structure. In fact, ultrathin films have previously been used in fundamental research on, e.g., heterogeneous catalysis or interactions of different biopolymers with each other, but the attention is usually targeted on catalytic phenomena[7] or adsorption,[8] not internal physical and/or chemical changes occurring within the film itself.[9] The insight provided by GISAXS on the acid regeneration of cellulose holds promise of an analytical practice that could be applied for many other biopolymer systems where various simple chemical and physical treatments induce crucial alterations in the supramolecular architecture.

The system applied in this study was an ultrathin film consisting of trimethylsilyl cellulose (TMSC, Figure 1a) which is being regenerated into cellulose by exposure to HCl vapor.[10] First, the regeneration process is investigated *in situ* by GISAXS. A spin-coated TMSC film of ∼51.9 nm initial thickness on a silicon wafer substrate is placed in a specially designed chemical reaction chamber[11] (Figure 1b): the lower compartment is equipped with a connection to a syringe pump filled with 3 M aqueous HCl, while the upper one is used for mounting the sample. The compartments are separated by a holey grid that enables HCl vapor created in the lower compartment to enter into the upper compartment, and a direct contact of the sample with the liquid is prevented. The vapor stream is further facilitated by a slight stream of N_2 gas through the chamber. Initially, GISAXS patterns are measured for 12 min on the as-prepared sample without HCl injections to gain information on initial film properties and to exclude beam damage. The parameter to directly emerge from GISAXS is an easy estimate of changes of the GISAXS pattern, the correlation length l_{CH}*, i.e., an estimate of the intensity-averaged electron density fluctuations throughout the whole film. The derived correlation length of 12.8 nm is nearly constant showing that the beam has negligible effect on the measurement (Figure 2a).

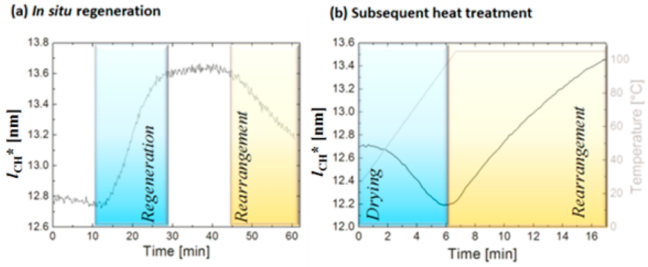

Figure 2. (a) Plot of the changes of the mean correlation length l_{CH}* over time during the regeneration process; blue indicates the TMS cleavage, whereas the yellow area shows the pore rearrangement. (b) Subsequent temperature treatment of regenerated cellulose film.

After injection of aqueous HCl, the created HCl vapors immediately induce the desilylation reaction of TMSC. It can be clearly seen (Figure 2a) that immediately after injection of the HCl into the cavity (t = 12 min) the reaction is initiated, which is accompanied by an increase in l_{CH}* until the film is completely converted to cellulose (t = 28 min). In principle, there are two main options why l_{CH}* of a film increases. Either the pores inside the film are getting larger or the distance between the pores increases, e.g., by densification of the thin film due to rearrangements within the material.

In fact, two processes occur simultaneously in the system. The silyl groups are cleaved off leading to voids between the cellulose chains. The subsequent densification of the film leads to an increase of the distance between those voids which should be reflected in an increase in l_{CH}*. However, it is known from the literature that the layer thickness of the films is significantly reduced during the regeneration procedure as shown by *ex situ* investigations with X-ray reflectivity (XRR, Figure 3). This shrinkage of the film is accompanied by the formation of inter- and intramolecular hydrogen bonds in the cellulose films.

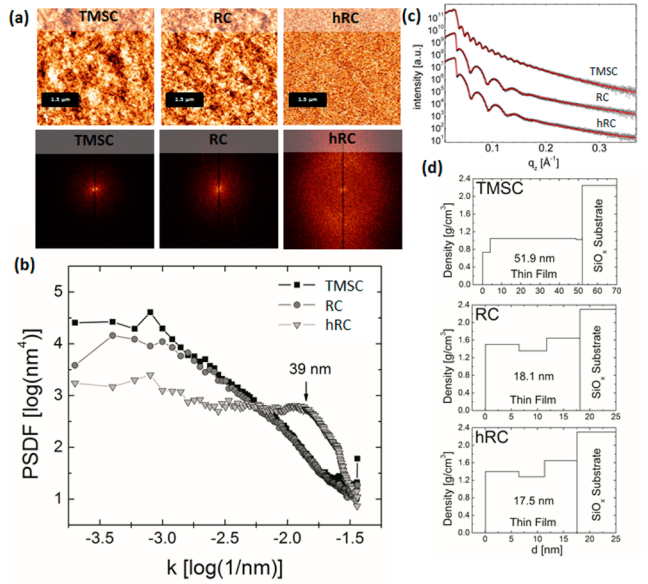

Figure 3. (a) AFM images of TMSC, regenerated cellulose (RC), and heated cellulose (hRC) with their corresponding 2D fast Fourier transformation. (b) Power spectral density function plot (PDSF) of AFM images shown in (a). (c) XRR study with model fits (red line) and (d) with the corresponding density plot for each thin film and film thickness.

DOI: 10.1021/acsmacrolett.5b00306
ACS Macro Lett. 2015, 4, 713−716

Consequently, the density is increased (from 0.99 to 1.50 g cm^{-3}, see Supporting Information (SI), Table S3). By contrast, an increase of l_{CH}* occurs, probably because not all of the voids created by cleaved TMS groups can be covered by hydrogen bonds, which can be seen as an increase of the distance between the remaining pores. This behavior may originate from the rather high molecular weight of the cellulose molecules, which prevents the film from achieving thermodynamic equilibrium within the time frame of the investigations.

For many regeneration processes involving biopolymers, the exposure time to regeneration agents is an important parameter for the resulting materials properties. Therefore, the effect of a further exposure to HCl vapors was investigated. After an additional 15 min exposure to HCl vapors, l_{CH}* starts to decrease, probably due to partial hydrolysis of the cellulose concomitant with higher mobility of the chains and more efficient hydrogen bonding. As a consequence of more efficient H-bonding, voids between the chains become smaller, and l_{CH}* decreases. The second investigated rearrangement here is water removal by heating. For these, the same films have been transferred to a temperature-controlled sample stage, which is operated under a steady flow of N_2. As depicted in Figure 2b, at a temperature of ca. 50 °C, l_{CH}* starts to decrease until reaching the target temperature of 105 °C which is commonly used in a variety of polysaccharide manufacturing processes. These changes can be interpreted as a more efficient interaction within and between cellulose molecules leading to smaller pores due to the collapse of capillary bridges. Interestingly, when the films are kept at 105 °C for an additional 10 min, l_{CH}* starts to increase again. At this stage, aggregation and fibrillation are initiated, as shown by AFM images (Figure 3a). The images and their power spectral density plots show that the regeneration procedure does not have any effect on the mesoscopic morphology of the films, whereas the heating eventually leads to the fibrillation resulting in correlation lengths in the range of 39 nm (Figure 3b), corresponding to the length scale most dominant over the whole investigated area (5 μm × 5 μm).

Additionally, XRR studies evaluated by a three-layer model fit (for details and justification see SI) clearly show that the layer thickness of the samples is reduced from 18.1 to 17.5 nm (3%) upon drying, indicating a tighter packing (Figures 3c and 3d). A tighter packing in turn may result in smaller pore size distributions, but here a clear increase of l_{CH}* (Figure 2b) is observed. This, however, is logical if one assumes the creation of larger nanogaps between the fibrils during the aggregation/fibrillation process that results in larger, more inhomogeneous domains at the nanoscopic level again. As a consequence, the fibrils themselves become denser, exhibiting decreased pore sizes, but the interfibrillar distances are getting larger, causing an overall increase of the l_{CH}*. At this point, it should be noted that crystallization does not take place as demonstrated earlier by grazing incidence diffraction experiments.[9b]

The importance of the results can be rationalized when considering the analogies that are present between our model system and other polysaccharides such as chitin. In the case of chitin, similar rearrangements take place upon regeneration and drying, but these are far less explored than in the case of cellulose originating from its rather low direct industrial use. Therefore, the described approach can be considered a generic tool to understand and to follow dynamic changes in a variety of polysaccharide-based materials, unreachable for many other sophisticated techniques. Solid-state NMR and IR spectroscopy, for instance, can be applied to study changes in crystallinity and hydrogen bonding patterns, but detailed insights into the resulting changes on the supramolecular level in terms of pore size changes remain inaccessible. Similarly, scattering experiments performed using lab X-ray sources feature the disadvantage of low scattering contrast, resulting in rather long acquisition times that make dynamic studies extremely difficult. The acquisition of BET isotherms, on the other hand, is performed *ex situ*; i.e., a drying procedure among others has been applied beforehand, which impedes the observation of dynamic effects during physical or chemical treatments. The outreach of the shown approach goes beyond the mere basic understanding of the behavior of thin films. For example, in many polysaccharide-based processes, derivatization steps are employed (e.g., xanthogenation) to enable efficient processing and subsequent regeneration. As demonstrated in this study, the regeneration procedure itself changed the pore structure and distribution, whereas the resulting cellulose film exhibits larger correlation lengths than the starting material despite a higher density of the material. Prolonged exposure to the regeneration agent led to a further decrease in l_{CH}*, presumably due to hydrolysis of cellulose, subsequent increased mobility of the chains, and more efficient hydrogen bonding. However, the l_{CH}* of the initial TMSC film was not reached even after extended exposure times to HCl vapors.

It is known that prolonged exposure of cellulose materials to regeneration baths induces depolymerization, which in turn causes a decrease in mechanical properties and a change in the haptics of the fibers. Therefore, the knowledge on what happens in the pores in our model system may also influence the understanding of fiber-making processes since the effect of the regeneration procedure on the pore size is generally not investigated *in situ*.[9b] Similarly, there is hardly any real-time, *in situ* information on the drying processes, often used in pulping, papermaking, and fiber processing. This study showed that the removal of water from the films expectedly led to a decrease in pore size (or distance between the pores) up to the target temperature of 105 °C which is one of the most commonly used drying procedures in industrial processes. Unexpectedly, however, a longer exposure to elevated temperature was accompanied by an increase in pore size, which is probably a consequence of mesoscopically observed aggregation into fibrils creating nanopores. Although many TGA/DSC investigations on real samples have been reported, they just give insight into water loss and potential decomposition processes, whereas sorption experiments are usually performed *ex situ*, making direct correlations to pore size changes difficult.

However, there are also limitations of the simplified surface-sensitive approach with GISAXS that essentially is restricted to observing fundamental phenomena within homogeneous amorphous films. Heterogeneity in morphology, chemical composition, and crystallinity naturally play a role in practical systems. Nevertheless, following the fundamental changes at the nanoscopic and mesoscopic level is a prerequisite to the basic understanding of the roles of all different contributions in the processes.

Finally, these results may complement also the recent discussion on the structural role of water in biological systems, determining the function, conformation, and molecular recognition of proteins for instance.[12] While for proteins the water interactions are usually investigated in the dissolved state, for cellulose-containing materials and many other biopolymer assemblies such as tissues, the relevant system consists of a

DOI: 10.1021/acsmacrolett.5b00306
ACS Macro Lett. 2015, 4, 713−716

hydrogel with lower ratios of water involved, which is addressed in this communication. For example, in nature the interplay of water, cellulose, and hemicelluloses is an important factor for the structural integrity of wood.[13] However, for a complete understanding of the rather complex interaction between water and cellulose and its impact on the properties of cellulose-based materials, a lot more work remains to be done, particularly on the computational and simulation levels.

■ ASSOCIATED CONTENT

Supporting Information

Experimental details and procedures are given (film preparation, analytical methods, GISAXS, XRR). The Supporting Information is available free of charge on the ACS Publications website at DOI: 10.1021/acsmacrolett.5b00306.

■ AUTHOR INFORMATION

Corresponding Authors

*H.E.: heike.ehmann@tugraz.at.
*E.K.: eero.kontturi@aalto.fi.
*S.S.: stefan.spirk@tugraz.at.

Notes

The authors declare no competing financial interest.
[¶](S.S.) Member of the European Polysaccharide Network of Excellence (EPNOE) and member of NAWI, Graz.

■ ACKNOWLEDGMENTS

This work was financially supported by the Austrian Research Promotion Agency (FFG) under grant agreement 842413 (Cello-H_2O-4papers). E.K. acknowledges Academy of Finland (grant no. 259500) for financial support. Elettra Sincrotrone is acknowledged for providing synchrotron radiation at the Austrian SAXS beamline.

■ REFERENCES

(1) Klemm, D.; Heublein, B.; Fink, H.-P.; Bohn, A. *Angew. Chem., Int. Ed.* **2005**, *44*, 3358.

(2) Zugenmayer, M. *Crystalline Cellulose and Cellulose Derivatives*; Springer-Verlag: Berlin-Heidelberg Germany, 2008.

(3) (a) Nishiyama, Y.; Johnson, G. P.; French, A. D. *Cellulose* **2012**, *19*, 319. (b) Nishiyama, Y.; Sugiyama, J.; Chanzy, H.; Langan, P. *J. Am. Chem. Soc.* **2003**, *125*, 14300. (c) French, A. D.; Concha, M.; Dowd, M. K.; Stevens, E. D. *Cellulose* **2014**, *21*, 1051. (d) Sugiyama, J.; Vuong, R.; Chanzy, H. *Macromolecules* **1991**, *24*, 4168. (e) Rossetti, F. F.; Panagiotou, P.; Rehfeldt, F.; Schneck, E.; Dommach, M.; Funari, S. S.; Timmann, A.; Müller-Buschbaum, P.; Tanaka, M. *Biointerphases* **2008**, *4*, 117. (f) Shen, T.; Langan, P.; French, A. D.; Johnson, G. P.; Gnanakaran, S. *J. Am. Chem. Soc.* **2009**, *131*, 14786. (g) Kono, H.; Yunoki, S.; Shikano, T.; Fujiwara, M.; Erata, T.; Takai, M. *J. Am. Chem. Soc.* **2002**, *124*, 7506.

(4) Fernandes, A. N.; Thomas, L. H.; Altaner, C. M.; Callow, P.; Forsyth, V. T.; Apperley, D. C.; Kennedy, C. J.; Jarvis, M. C. *Proc. Natl. Acad. Sci. U.S.A.* **2011**, *108*, E1195.

(5) (a) Petridis, L.; O'Neill, H. M.; Johnsen, M.; Fan, B.; Schulz, R.; Mamontov, E.; Maranas, J.; Langan, P.; Smith, J. C. *Biomacromolecules* **2014**, *15*, 4152. (b) Driemeier, C.; Bragatto, J. *J. Phys. Chem. B* **2013**, *117*, 415.

(6) (a) Chundawat, S. P. S.; Bellesia, G.; Uppugundla, N.; da Costa Sousa, L.; Gao, D.; Cheh, A. M.; Agarwal, U. P.; Bianchetti, C. M.; Phillips, G. N., Jr.; Langan, P.; Balan, V.; Gnanakaran, S.; Dale, B. E. *J. Am. Chem. Soc.* **2011**, *133*, 11163. (b) McKee, J. R.; Appel, E. A.; Seitsonen, J.; Kontturi, E.; Scherman, O. A.; Ikkala, O. *Adv. Funct. Mater.* **2014**, *24*, 2706. (c) Wolfberger, A.; Petritz, A.; Fian, A.; Herka, J.; Schmidt, V.; Stadlober, B.; Kargl, R.; Spirk, S.; Griesser, T. *Cellulose* **2015**, *22*, 717. (d) Kelly, J. A.; Giese, M.; Shopsowitz, K. E.; Hamad, W. Y.; MacLachlan, M. J. *Acc. Chem. Res.* **2014**, *47*, 1088. (e) Montrikittiphant, T.; Tang, M.; Lee, K.-Y.; Williams, C. K.; Bismarck, A. *Macromol. Rapid Commun.* **2014**, *35*, 1640.

(7) Somorjai, G. A.; Frei, H.; Park, J. Y. *J. Am. Chem. Soc.* **2009**, *131*, 16589.

(8) (a) Kargl, R.; Mohan, T.; Köstler, S.; Spirk, S.; Doliska, A.; Stana-Kleinschek, K.; Ribitsch, V. *Adv. Funct. Mater.* **2013**, *23*, 308. (b) Orelma, H.; Teerinen, T.; Johansson, L.-S.; Holappa, S.; Laine, J. *Biomacromolecules* **2012**, *13*, 1051. (c) Kontturi, E.; Tammelin, T.; Österberg, M. *Chem. Soc. Rev.* **2006**, *35*, 1287.

(9) (a) Kontturi, E.; Suchy, M.; Penttilä, P.; Jean, B.; Pirkkalainen, K.; Torkkeli, M.; Serimaa, R. *Biomacromolecules* **2011**, *12*, 770. (b) Mohan, T.; Spirk, S.; Kargl, R.; Doliska, A.; Vesel, A.; Salzmann, I.; Resel, R.; Ribitsch, V.; Stana-Kleinschek, K. *Soft Matter* **2012**, *8*, 9807.

(10) (a) Kontturi, E.; Thüne, P. C.; Niemantsverdriet, J. W. *Langmuir* **2003**, *19*, 5735. (b) Schaub, M.; Wenz, G.; Wegner, G.; Stein, A.; Klemm, D. *Adv. Mater.* **1993**, *5*, 919.

(11) Sinturel, C.; Grosso, D.; Boudot, M.; Amenitsch, H.; Hillmyer, M. A.; Pineau, A.; Vayer, M. *ACS Appl. Mater. Interfaces* **2014**, *6*, 12146.

(12) Nibali, V. C.; Havenith, M. *J. Am. Chem. Soc.* **2014**, *136*, 12800.

(13) Suchy, M.; Virtanen, J.; Kontturi, E.; Vuorinen, T. *Biomacromolecules* **2010**, *11*, 515.

DOI: 10.1021/acsmacrolett.5b00306
ACS Macro Lett. 2015, 4, 713−716